

# The Right Ventricle: A Comprehensive Review From Anatomy, Physiology, and Mechanics to Hemodynamic, Functional, and Imaging Evaluation

Anita Sadeghpour,<sup>1</sup> and Azin Alizadehasl<sup>1,\*</sup>

<sup>1</sup>Rajaie Cardiovascular Medical and Echocardiography Research Center, Iran University of Medical Sciences, Tehran, IR Iran

\*Corresponding author: Azin Alizadehasl, Rajaie Cardiovascular Medical and Echocardiography Research Center, Vali-Asr St., Tehran, IR Iran. Tel/Fax: +98-2123922190, E-mail: alizadeasl@gmail.com

Received 2015 September 01; Revised 2015 October 15; Accepted 2015 November 15.

## Abstract

The right ventricle (RV) is a complex structure with abstruse function that reveals important differences when compared to the left ventricle (LV), so it cannot be described as a simple geometric form and achromatic physiology. As an inference from this fact, in the present review, we aim to describe RV structure including the embryology, anatomy, and physiology and present a functional, hemodynamic, and imaging assessment of the normal and failing RV. So that, we conducted a thorough review based on the database sources such as MEDLINE, PubMed, Cochrane and Google scholar. No restrictions were placed on study date, study design, or language of publication. We searched all valuable and relevant information considering the anatomy, physiology, mechanics, hemodynamic and imaging evaluation of RV.

**Keywords:** Right Ventricular Anatomy, Right Ventricular Physiology, Right Ventricular Mechanics, Right Ventricular Hemodynamic, Right Ventricular Function, Right Ventricular Imaging

## 1. Introduction

The facts about the role of the right ventricle (RV) in health and disease in history have lagged behind those of the left ventricle (LV). Previously, the RV was considered a transmitting chamber with no hemodynamic effect in cardiac output in the normal heart and as a victim or a mere bystander in the diseased heart. Less muscle, it was believed, restricted its role to pumping blood through a single organ and it was less commonly or noticeably involved than was the LV in diseases of epidemic proportions such as cardiomyopathy, valvulopathy, and myocardial ischemia. Nonetheless, even the proportionately limited evidence relating to RV function, its damage in various disease states, and its influence on the outcome of those diseases and abnormalities suggests that the RV is a significant contributor and that further understanding of these issues is of essential importance (1-3).

In the first half of the 20th century, the assessment of RV function was limited to a small group of researchers interested by the hypothesis that human circulation could function sufficiently without RV contractile function. Their research, however, was based on animal studies. Since then, the importance and implication of RV function has been recognized in RV myocardial infarction, heart failure, congenital heart disease, and also pul-

monary hypertension. More recently, significant advances in echocardiography and also magnetic resonance imaging (MRI) have generated new chances for the study of RV anatomy, hemodynamic, physiology, and function. RV chamber is affected by and contributes to a number of diseases, including most remarkably pulmonary hypertension caused by a variety of lung or pulmonary vascular diseases (cor pulmonale). Other diseases affect the RV in different ways, including global, LV, or RV-specific cardiomyopathies; RV ischemia or infarction; pulmonary or tricuspid valvular heart disease; and also left-to-right shunts (1, 4-6).

## 2. Evidence Acquisition

### 2.1. Embryology

A basic understanding of embryology is useful in the study of cardiovascular and congenital heart disease. The RV and RV outflow tract are derived from the anterior heart field, while the LV and the atrial chambers are derived from the primary heart field.

The sinus part of the RV is derived from the ventricular portion of the primitive cardiac tube, while the infundibulum of the RV is derived from the conus cordis. Under normal conditions, the dextroventricular loop places the anatomic RV to the right and the anatomic LV to the left;

nevertheless, the complex spiral development of the outflow tracts explains the characteristic crisscross relationship between the right and left outflow tracts, with RV outflow tract being located anteriorly and to the left of LV outflow tract (1, 6-9).

## 2.2. Anatomy

Whereas the LV is conical, the RV is more triangular and semilunar in form on vertical plans. The RV differs from the LV in that the former has strict trabeculae, a moderator band, and inter-valve fibrous tissues. Interestingly, the muscle mass of the RV is about one-sixth that of the LV. This could be described by different loading conditions of the ventricles. The RV pumps the same stroke volume as does the LV, but with about 25% of the stroke work due to the low resistance of the pulmonary vasculature. So, by virtue of the Laplace rule, the RV is more thin-walled (3 - 4 mm) and also compliant.

The geometry of the chamber is more complex, containing of an inlet (sinus) section and an outlet (conus) portion separated by the crista supraventricularis. Longitudinal shortening is a greater and more important contributor to RV stroke volume than is circumferential shortening. The RV is linked to the LV in several ways: by a shared wall (via the septum), by reciprocally encircling epicardial fibers, by sharing the pericardial space, and by the attachment of RV free wall to the anterior and posterior septum. The blood supply of RV free-wall is mainly from the right coronary artery (RCA) and almost receives an equal flow during systole and diastole. The left anterior descending coronary artery (LAD) supplies the anterior two-thirds of the septum, and the posterior descending artery (PDA) supplies the one-third of the inferoposterior portion of the septum (1-3, 6)

In the normal heart, the RV is the most anteriorly located cardiac chamber and lies closely behind the sternum. The RV can be defined in terms of 3 components: a, the inlet, which consists of the tricuspid valve, chordae tendineae, and papillary muscles; b, the trabeculated apical myocardium; and c, the infundibulum or conus, which corresponds to the smooth myocardial outflow section.

The shape and structure of the RV is complex. In contrast to the ellipsoidal shape of the LV, the RV looks triangular when viewed from the side section and crescent-shaped when watched in cross-section. The shape of the RV is also affected by the position of the interventricular septum. Under normal loading and electrical situations, the septum is concave toward the LV in both systole and diastole Figure 1A, 1B (6, 8, 9)

## 2.3. Myofibers of the Right Ventricle

Both ventricles are not composed of a single muscle layer but rather of several layers that form a 3-dimensional (3D) network of fibers. As was described by Ho and Nihoyannopoulos (9) RV wall is principally composed of superficial and also deep muscle layers. The fibers of the superficial layer are arranged circumferentially in a direction that is parallel with the atrioventricular groove. These fibers turn obliquely toward the cardiac apex and continue into the superficial myofibers of the LV. However, the deep muscle fibers of the RV are longitudinally aligned from base to apex. In contrast to the RV, the LV comprises obliquely oriented myofibers superficially, longitudinally oriented myofibers in the subendocardium, and mainly circular fibers in between them. This arrangement contributes to the more complex movement of the LV which contains torsion, translation, rotation, and also thickening.

The continuity between the muscle fibers of the RV and LV functionally binds the 2 ventricles together and represents the anatomic basis of RV free-wall traction caused by LV contraction. This continuity also contributes, along with the interventricular septum, to ventricular interdependence (1, 6, 8, 9).

## 2.4. Genetic and Cellular Biology of the Right Ventricle

The genetic study of cardiac morphogenesis has shown that the RV and the LV originate from different progenitor cells and different sites. The primary heart field gives rise to the atrial chambers and the LV, while the cells of the anterior heart field develop into RV outflow tract and the RV. The transcription factor Bop as a regulator of the development of the RV is now known to be a transcriptional target of myocyte enhancer factor 2C and GATA4 is mandatory for HAND2 expression, which is necessary for the formation of the RV. GATA4 regulates the cardiac muscle-specific expression of the  $\alpha$ -myosin heavy chain gene and also the gene encoding atrial natriuretic factor.

The degree of RV hypertrophy in idiopathic pulmonary arterial hypertension (PAH), measured as RV free-wall thickness, is highly variable (0.6 to 1.5 cm) and, as in the failing LV, there is evidence for changes of gene expression in the pressure overloaded failing RV in patients with idiopathic PAH. Particularly, it appears that there is a recapitulation of the fetal gene pattern with a decline in the  $\alpha$ -myosin heavy chain gene and an increase in the expression of the fetal  $\beta$ -myosin heavy chain.

Clinical experience shows that some patients with cardiomyopathy or PAH develop RV failure earlier than do others as evaluated by RV filling pressures and cardiac output at the time of diagnosis. It has also been suggested that there might be a genotypic difference between patients:

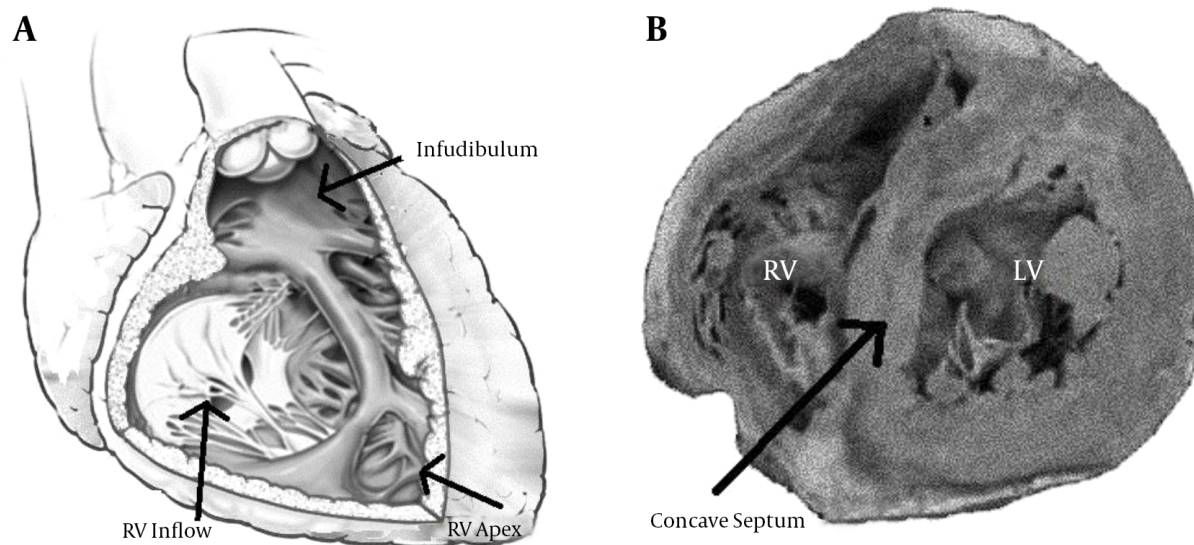


**Figure 1.** A, The inlet, trabeculated apical myocardium and infundibulum of the RV; B, Concave interventricular septum.

Some patients develop greater hypertrophy (thicker free wall) of the RV for the same degree of afterload than do others. A small cohort study of patients with idiopathic PAH showed that patients with the angiotensin-converting enzyme DD polymorphism had a normal right atrial (RA) pressure and cardiac output, whereas the non-DD patient group had an increased RA pressure and a decreased cardiac output. While it is unlikely that this polymorphism alone can explain differences in the degree of RV hypertrophy between patients, this observation posits the concept of genetically controlled RV hypertrophy (1, 9-15).

### 2.5. Hemodynamics and Mechanics

RV contraction is sequential, beginning with the contraction of the inlet and trabeculated myocardium and ending with the contraction of the infundibular portion (nearly 25 to 50 ms apart). Of course, the contraction of the infundibulum is of a longer duration than is the contraction of the inflow region.

The RV contracts by 3 separate tools: a, inward movement of the RV free wall, which creates a bellows effect; b, contraction of the longitudinal myofibers, which shortens the long axis and pulls the tricuspid annulus toward the apex; and c, traction on the free wall at the points of attachment secondary to LV contraction. Moreover, because of the higher surface-to-volume ratio of the RV, a smaller inward motion can eject the same stroke volume. The quantitation of RV volumes (end-diastolic and end-systolic) is slightly greater than that of LV volumes, resulting in a

mildly reduced ejection fraction (EF) in the RV compared to the EF in the LV.

In normal conditions, right-sided pressures are meaningfully lower than are comparable left-sided pressures. RV pressure tracings display an early peaking and a rapidly lessening pressure in contrast to the rounded contour of LV pressure tracing. Also, RV isovolumic contraction time is shorter because RV systolic pressure quickly exceeds the low pulmonary artery diastolic pressure. A cautious study of hemodynamic tracings and flow dynamics also shows that the end-systolic flow might continue in the presence of a negative ventricular-arterial pressure gradient.

RV free wall contains mainly circumferential-oriented myofibers in the subepicardium and longitudinal myofibers in the subendocardium and lacks the middle layer. Regarding the longitudinally arranged subendocardial myofibers in RV free wall, RV contraction is more longitudinal than it is circumferential. This myofiber arrangement of the RV would not support the concept of RV torsion; however, RV torsion has been suggested in some studies (1, 6, 8, 16-18).

Despite all the above-mentioned explanations, the mechanisms by which LV failure can lead to RV dysfunction are only partly understood. Congestive heart failure adversely affects lung mechanics and also gas exchange. Pulmonary function abnormalities contain a reduction in lung volumes with reduced lung compliance. Though this restrictive lung physiology is improved in some degree by fluid removal or after heart transplantation, the reduced alveolar-capillary membrane diffusing capacity is

not changeable and reversible demonstrating the clinical importance of lung structural remodeling in congestive heart failure.

The lungs from animal models of congestive heart failure as well as from humans with pulmonary venous hypertension reveal septal thickening with myofibroblast proliferation and also interstitial matrix deposition. The physical and biological determinants of these changes and their subsequent effects on the development of RV failure are presently unknown (1, 8, 9).

#### 2.6. Perfusion of the Right Ventricle

The RV has its unique and matchless blood supply system. It is a part of the overall coronary circulation containing of coronary arteries originating from the ascending aorta. They have small branches that dive into the heart muscle to bring it blood. The blood supply of the RV differs according to the predominance of the coronary system. In a right-dominant system, found in about 80% of the population, the RCA supplies most of the RV. The lateral wall of the RV is supplied by the marginal branches of the RV, while the posterior wall and the inferoseptal region are supplied by the PDA. The anterior wall of the RV and the anteroseptal region are supplied by branches of the LAD. The infundibulum derives its supply from the conal artery, which has a separate ostial origin in 30% of cases (1, 5, 6). The RCA provides blood to the atria with small blood vessels. In about 50% of patients, the proximal RCA gives rise to the sinus node artery. Originating from the single short ostium a short, common LCA trunk branches into the LAD and the left circumflex artery (LCX). Running in the anterior interventricular groove, the LAD gives rise to the anterior septal perforating branches to supply blood to the cardiac apex. The other small branches of the LAD supply the anterior wall of the RV, and the diagonal branches supply the anterolateral free wall of the LV. The LCX courses within the posterior groove, around the obtuse margin, and posteriorly toward the crux of the heart. In about 10% of patients, the LCX reaches the crux of the heart and supplies the PDA (left domination form). The atrial branches may arise from the LCX and supply the sinus node in 40% of patients. Before turning toward the diaphragmatic surface of the heart, the RCA gives rise to the right marginal branch, which runs along the right margin, to supply the wall of the RV. Again, the RCA gives rise to several more branches like the conus branch and the sinus node artery, passing upward to the auricle wall to the junction between the superior vena cava, sulcus terminals, and right auricle.

In the absence of severe RV hypertrophy or pressure overload, proximal RCA flow happens during both systole and diastole. Nonetheless, beyond the marginal branches of the RV, the diastolic coronary blood flow dominates. The

relative resistance of the RV to irreversible ischemic damage may be described by 1, its lower oxygen consumption; 2, its more extensive collateral system particularly from the moderator band artery, a branch of the first septal perforator that originates from the LAD artery; and 3, its ability to raise oxygen extraction (6-9).

#### 2.7. Ventricular Interdependence

Ventricular interdependence is most apparent with changes in loading conditions such as those seen with respiration or sudden postural changes. Ventricular interdependence plays an essential role in the pathophysiology of RV failure and dysfunction.

Systolic ventricular interdependence is mediated chiefly through the interventricular septum. The pericardium might not be as important for systolic ventricular interdependence as it is for diastolic ventricular interdependence. Experimental animal studies have shown that about 20% to 40% of RV systolic pressure and stroke volume results from LV contraction. Furthermore, in the presence of scar formation in the RV or even replacement with a non-contractile patch, the septum is able to keep circulatory stability as long as the RV is not dilated.

The evidence for diastolic ventricular interdependence is well recognized and based on many animal, experimental, and clinical studies. In acute RV pressure or volume overload states, the dilatation of the RV shifts the interventricular septum toward the left, changes LV geometry, and increases the pericardial constraint. As a result, LV diastolic pressure-volume curve shifts upward (reduced dispensability), which potentially leads to a declined LV preload, an increased LV end-diastolic pressure (typically a mild increase), or low cardiac output states. Acute RV dilatation has also been revealed to lead to a decline in LV elastance (1, 9, 17, 19).

#### 2.8. Right Ventricle in Volume Overload Conditions

Although the severity of tricuspid regurgitation correlates with worse survival, the RV tolerates volume overload better than pressure overload and may, therefore, remain well-adapted to right-sided valvular regurgitant lesions for extended periods of time. Likewise, in pulmonary hypertension associated with initial left-to-right shunting, the lesion might remain minimally symptomatic during the high-volume phase until pulmonary vasculopathy develops and the shunt reverses (the Eisenmenger phenomenon). Even after the Eisenmenger physiology is well established, the outlook for these patients is better than that for patients with idiopathic PAH, maybe because of preconditioning by the prior volume load or the retaining of fetal right-heart phenotype characteristics (1, 2, 6-9).



### 2.9. Right Ventricle in Pulmonary Hypertension

In all forms of pulmonary hypertension, RV function remains the main hemodynamic factor for survival. Although the prognosis of patients with PAH and chronic thromboembolic pulmonary hypertension improves with the development of more effective medical and surgical managements, our understanding of the factors that define how the RV responds to pulmonary hypertension remains incomplete. For example, it is not clear why some patients are able to adapt to and tolerate very high pulmonary artery pressures, while others with similar or even less significant pressures progress to RV failure and die in a low cardiac output state.

A preliminary adaptive reaction in the form of myocardial hypertrophy is followed by progressive contractile dysfunction. RV dilatation ensues to allow compensatory preload and keep stroke volume despite reduced fractional shortening. As contractile weakening progresses, clinical evidence of decompensated RV failure happens characterized by rising filling pressures, diastolic dysfunction, and diminishing cardiac output which is compounded by tricuspid regurgitation due to annular dilatation and the resultant poor leaflet coaptation. The increased size and pressure overload of the RV also create diastolic dysfunction in the LV. Therefore, not only are the function and size of the RV indicators of the severity and chronicity of pulmonary hypertension, but also they impose additional symptoms and reduce longevity. Finally, RV function is the most important factor of longevity in patients with PAH (8, 9, 20-24).

The specific mechanisms and tools underlying the development of RV failure secondary to pulmonary hypertension are unclear and uncertain. For example, it is unclear whether some patients develop RV myocardial ischemia, whether there is microvascular endothelial cell dysfunction, and whether or not myocytes experience apoptosis. In severe, end-stage pulmonary hypertension, the shape and contour of the RV is changed from the normal conformation and RV wall stress and also RV free-wall thickness seem inversely correlated. The mechanism and tool by which a severely dilated end-stage RV repairs itself after lung transplantation is also uncertain and unclear.

The plasma levels of brain natriuretic peptide and troponin T associate with pulmonary artery pressure and pulmonary vascular resistance in patients with PAH. Rises in brain natriuretic peptide plasma levels during serial follow-up visits are correlated with increased mortality in patients with idiopathic PAH. Paradoxically, atrial natriuretic peptides could promote cardiomyocyte survival.

Echocardiography and cardiovascular magnetic resonance (CMR) imaging allow noninvasive assessment of RV function and also structure, and a number of indices have

been revealed to have a significant potential prognostic value in PAH. Given the significance of the RV in PAH, preservation or improvement of its function must constitute important aspects of therapy. Nonetheless, there are currently limited data specifically associated with this aspect of management response. Simple, reproducible, non-invasive measures of RV function would help improve the treatment of patients with PAH and provide tools to assist in the creation of the optimal therapeutic approach not only to manage the effects of the disease on the heart and pulmonary vasculature but also to augment and support RV function (1, 9, 16, 21-26).

Two-dimensional (2D) echocardiography is inexpensive, portable, and convenient. It is most commonly used for the detection of suspected pulmonary hypertension in a symptomatic individual and also has a role in establishing an underlying cause (e.g., LV dysfunction and intracardiac shunt). In patients with an established diagnosis, 2D echocardiography is commonly used to assess and monitor biventricular function, valvular function, inferior vena cava dimensions, and pericardial effusion. Pulmonary artery pressure can be derived noninvasively using a simplified version of the Bernoulli equation. In the absence of pulmonary valve stenosis, systolic pulmonary artery pressure =  $4v$  (peak tricuspid valve jet velocity) (2) + estimated RA pressure. RA pressure can be estimated by various methods, including the inferior vena cava collapsibility index and the height of the jugular venous pressure on clinical examination.

Intravenous contrast administration during 2D echocardiography can enhance faint Doppler tricuspid flow signals and assist in noninvasive pressure estimation. Contrast echocardiography can also be employed to detect intracardiac shunts and improve endocardial border delineation in patients with suboptimal acoustic windows.

Three-dimensional echocardiography eliminates the need for geometric assumptions and provides direct and more accurate measurements of RV volumes and systolic function than do 2D measurements.

Also, 2D speckle-tracking echocardiography (STE) and tissue Doppler imaging (TDI) allow the measurement of global and regional myocardial velocity and strain. Measurements are most commonly made of RV free wall. These values have been shown to correlate with RV systolic function and invasive pulmonary hemodynamics in patients with pulmonary hypertension and survival in patients with symptomatic heart failure too.

On the other hand, based on these proven capabilities, CMR imaging is currently the accepted gold standard method for assessing RV structure and function in patients with pulmonary hypertension (21-32).

### 2.10. Infarcted Right Ventricle

RV infarction may create sufficient myocardial damage to result in heart failure, arrhythmias, shock, and death in the absence of any superimposed volume or pressure overload and even unrelated to the extent of LV damage and myocardial loss. The occurrence of hemodynamic and symptomatic RV failure in these circumstances suggests that although the circulation can be maintained adequately when the RV is bypassed (as in properly selected patients undergoing a Fontan procedure), it is more prone to deterioration when there is a defective RV. Therefore, the enlarged hypocontractile RV seems to play an active role in compromising overall circulatory function. Whether this issue is due to ventricular interdependence and interaction, restrictive physiology, septal involvement, or other mechanisms has yet to be fully elucidated (33-35).

### 2.11. Arrhythmia

Cardiac rhythm plays a critical role in RV function. For example, atrial fibrillation can severely compromise RV function. In addition, ventricular tachycardia can originate from the RV in a variety of disorders such as arrhythmogenic RV dysplasia, idiopathic ventricular tachycardia, RV myocardial infarction, and left bundle-branch block as well as after surgical repair of congenital heart disease. Though a ventricular tachycardia that arises from the RV usually has a left bundle-branch block morphology, most ventricular tachycardias with this morphology rise from a paraseptal LV location (1, 2, 8, 9).

### 2.12. Right Ventricular Failure

RV failure, defined as incapability to maintain stroke volume, can happen when at least 1 of the 3 determining factors namely contractility, preload, and afterload is altered beyond physiological limits. Due to the functional interdependence of the ventricles, LV failure might have an additional negative effect.

Myocardial infarction involving the RV is a common reason for RV contractile dysfunction. Although the myocardium of the RV may be more protected against ischemia than is the myocardium of the LV, RV infarction alone may result in severely hemodynamic impairment and death. RV myocardial infarction happens when the RCA has a proximal occlusion and accompanies up to 50% of inferior myocardial infarctions. The decline in contractile function after RV infarction reduces the preload for the LV, which results in a lower cardiac output in the systemic circulation. Additionally, RV ischemia damages LV filling due to direct ventricular interaction, especially when the pericardium is intact. Similarly, later RV dilation can have direct detrimental effects on LV function.

Severe pulmonary embolism creates an acute afterload increase. The function of the thin-walled RV is matched to a low resistance circulation and has insufficient adaptive capacity in such an event. The mechanism of RV failure is, thus, subendocardial ischemia followed by an inflammation process.

A chronic increase in afterload, such as chronic pulmonary hypertension, activates molecular adaptive mechanisms that stimulate the hypertrophy of RV free wall. In tandem with a more rounded shape, which increases curvature, these adaptive mechanisms reduce wall stress and allow the maintenance of the normal cardiac output. In the long run, however, a chronic afterload increase will result in decreased contractility and dilatation: a vicious circle with further RV remodeling and functional deterioration. The flatter septum reduces the contribution of the LV to the performance of the RV and has an additional detrimental negative effect. Increased preload is better tolerated by the RV, but it could finally also reduce patient survival. The most frequent conditions correlated with RV volume overload are tricuspid regurgitation, atrial septal defect, and pulmonary regurgitation (1-5, 34-36).

### 2.13. Right Ventricle in Left-Sided Heart Failure

#### 2.13.1. RV Dysfunction Can Develop in Patients With LV Dysfunction by Multiple Ways

- 1, LV failure increases afterload by increasing pulmonary venous and finally pulmonary artery pressure, partially as a protective mechanism in contrast to pulmonary edema;
- 2, the same cardiomyopathic process might concurrently affect RV chamber;
- 3, sometimes myocardial ischemia can involve both LV and RV;
- 4, LV dysfunction may lead to a reduced systolic driving pressure of RV coronary perfusion, which might be a substantial cause of RV function;
- 5, ventricular interdependence because of septal dysfunction may happen;
- 6, LV dilation in a limited pericardial box or compartment can restrict RV diastolic function.

On the other hand, RV pressure overload may happen with pulmonary hypertensive situations and compromise LV function, leading to parallel evidence of LV failure like pulmonary edema or pleural-pericardial effusion.

Given the multiple factors influencing RV function due to LV failure, RV status may be deemed a common final pathway in the development of congestive heart failure and, consequently, may be a sensitive indicator of impending decompensation and also poor prognosis.

In patients with advanced heart failure, RV shortening is the very significant independent associate of survival in multivariate analysis. Patients with RV shortening < 1.25 cm have a meaningfully worse survival over 2 years. But pa-

tients with acceptable RV function (RVEF > 35%) in the situation of severe heart failure have improved survival and also better exercise capacity. Indeed, in some studies, RVEF associates better with exercise capacity than does LVEF (1, 2, 6, 8, 9, 18, 19).

### 3. Results

#### 3.1. Right Ventricular Imaging

Different imaging techniques can be used to image the RV. Due to technological advances, the role and clinical use of these techniques is evolving. In different situations, each technique provides complementary and helpful information, which influences its use in the clinical setting. Presently, echocardiography and CMR imaging are the 2 most generally used imaging modalities for the structural and functional assessment of the RV. CMR is the reference standard method, and echocardiography is the most frequently utilized imaging modality for the assessment of RV size and systolic function.

Other imaging techniques such as cardiac computed tomography (CCT) and radionuclide techniques are valued alternatives in selected patients.

Since RV volume and function have a prognostic importance in different cardiac diseases (e.g., valvular heart disease, pulmonary hypertension, congenital heart disease, and heart failure), these imaging modalities should be validated by in vitro models and CMR as the gold standard method. Multimodality comparison studies between CMR, CCT, and 3D echocardiography have demonstrated a high correlation between 3D echo, CCT and RV volume measurements in CMR as the reference method. CCT volumetric measurements have shown slight (4%) overestimation and 3D echocardiographic measurements have revealed small underestimation, which shows that these imaging modalities are not interchangeable and serial assessments should be done by the same modality (3, 6, 19, 35-38).

#### 3.2. Echocardiography

RV morphology and structure can be sufficiently described by transthoracic echocardiography (TTE) in most patients. Indeed, when TTE imaging windows are poor and RV disease is assumed, additional imaging modalities such as transesophageal echocardiography (TEE), CMR, and CCT are required based on the patient's age and clinical problem. A study of RV size and function must be a part of every echocardiographic examination at the time of first diagnosis and during follow-up, mainly in patients with chronic conditions like PAH or cardiomyopathy.

Many studies have suggested that 2D TTE is not sufficiently accurate for the quantification of RV volumes. However, there has been a good correlation between CMR and 3D echocardiography in evaluating RV volumes and EF in selected populations (37).

Guidelines published for the echocardiographic assessment of the RV, point to the significance of combining different 2D echocardiographic views to gain full coverage of all the different RV segments, however, the normal data need stratifying for age ranges, body surface size, and gender (38-41).

Qualitatively, the RV should not be more than two-thirds of the LV in the apical 4-chamber view. When the RV becomes apex-forming, the RV is at least moderately enlarged and if the RV grows larger than the LV, it is significantly enlarged.

All different apical views as well as subcostal and parasternal long-axis and short-axis views should be obtained. Echocardiographic assessment should also include 2D measurements of RA dimensions and also RV wall thickness, which normally is < 0.5 cm (40, 41).

Assessment of RV volumes using 2D echocardiography is more challenging. In addition, 2D measurements of the RV as well as different geometrical formula suggested for volume calculation display a poor agreement with 3D volumes calculated by CMR. Of course, recently, 3D echocardiography has emerged as a promising technique for the evaluation of RV volumes. The most espoused method for the analysis of 3D volumetric data is the Beutel technique. This technique has been established to be reliable and also accurate in different situations, including congenital heart disease and PAH. The main limitation of this method is that it fails to confer good quality full volumetric 3D data, containing RV anterior wall and RV apical lateral segments especially in a dilated RV (36, 37, 40, 42)

Multiple parameters can be drawn upon in the assessment of RV systolic function globally such as fractional area change (FAC), RV index of myocardial performance (RIMP), RV 3D EF, RV strain, and strain rate (SR) or regionally such as tricuspid annular plane systolic excursion (TAPSE), peak tissue Doppler systolic velocity in the tricuspid annulus ( $S'$ ), and RV  $dP/dt$ .

The fact that the combined use of 3 different parameters (FAC, TAPSE, and RIMP) has been proposed may indicate that no single measurement has been authorized for clinical use and management and outcome. Given all the limitations discussed above, echocardiographic assessment of RV function remains challenging in clinical practice and is frequently limited to only qualitative assessment. Of course, recent guidelines have suggested performing quantitative measurements of RV function by using at least 1 of the following echocardiographic param-

ters:

### 3.2.1. Fractional Area Change

Fractional area change (FAC) is an independent and valid predictor of outcome after myocardial infarction and has been shown to correlate with RVEF measured by CMR. The RV FAC = end diastolic area (EDA)/end systolic area (ESA)/EDA  $\times$  100. A cutoff value  $<$  35% shows RV systolic dysfunction (Figure 2A and 2B) (40, 41).

### 3.2.2. Tricuspid Annular Plane Systolic Excursion

TAPSE is a simple, easy, and reproducible parameter. Less dependent on optimal image quality, TAPSE is angle-dependent and influenced by cardiac translation (Figure 3A). The presence of tricuspid regurgitation might influence the values obtained. TAPSE represents the longitudinal shortening of RV lateral wall (regional assessment capability) with limited normal standards for different age groups. However, minor variations based on gender and body surface area have been suggested. TAPSE  $<$  17 mm is highly suggestive of RV dysfunction. Although TAPSE is a one dimensional parameter, it enjoys a good correlation with RV FAC and radionuclide measurement of RVEF (39-41).

### 3.2.3. Peak Tissue Doppler Systolic Velocity in the Tricuspid Annulus

S' is a tissue Doppler-based method that evaluates RV longitudinal function (Figure 3B). This method is easy and reproducible but angle- and load-dependent and influenced by global cardiac translation. In the young adult, a normal cutoff value  $\geq$  11 cm/s has been proposed; however, based on the guidelines, S' velocity  $<$  10 cm/s and  $<$  9.5 cm/sec indicates RV systolic dysfunction. Moreover, S' has been shown to correlate well with the other measures of global RV systolic function (39-41).

### 3.2.4. Right Ventricular Index of Myocardial Performance

RIMP is a nongeometric index of global RV function. It is the ratio of the isovolumic time intervals (isovolumic contraction and relaxation times) to ventricular ejection time. The normal value of  $0.28 \pm 0.04$  has been suggested, which increases in the presence of RV systolic or diastolic dysfunction. It can be measured by either pulsed-wave Doppler study or TDI (tissue Doppler imaging) of the lateral tricuspid valve annulus, Figure 4. The cutoff values  $>$  0.43 for pulsed-wave Doppler-based RIMP and  $>$  0.54 for TDI indicate RV dysfunction. Recently, pseudonormalized values of RIMP in acute and severe RV myocardial infarction have been suggested, which can probably be explained by a decrease in isovolumic contraction time cor-

related with an acute increase in RV diastolic pressure and elevated RA pressure (5, 6, 39-48).

A  $dP/dt >$  400 mm Hg/sec strongly denotes a normal RVEF with a positive predictive value of 91%, sensitivity of 74%, and specificity of 84% for a normal RVEF when compared with CMR (49, 50).

The correlation between RV  $dP/dt$  and RV systolic function as well as functional capacity has been suggested in different studies. Nevertheless,  $dP/dt/V_{max}$  increases this correlation (49-51), (Figure 5).

### 3.2.5. Right Ventricular Diastolic Function

A variety of acute and chronic heart diseases, including volume and pressure overload, have been associated with RV diastolic dysfunction. LV diastolic assessment is relatively similar to the left-sided assessment by using the following parameters: pulsed-wave Doppler study of the tricuspid flow (E and A velocity and E/A ratio), TDI of the tricuspid annulus, IVRT, and deceleration time (39, 40, 52-54). Impaired relaxation has been defined by an E/A ratio  $<$  0.8, pseudonormal filling is defined when E/A ratio is 0.8 to 2.1 with an E/em ratio  $>$  6, and restrictive filling is defined when tricuspid E/A ratio is  $>$  2.1 with a deceleration time  $<$  120 ms (41).

## 3.3. Deformation of the Right Ventricle

### 3.3.1. Strain and Strain Rate Analysis

Strain and strain rate (SR) imaging is a well-established method for the quantification of regional and global myocardial function. Longitudinal strain is determined by the percentage of RV free-wall systolic shortening, while SR is the speed of this shortening. STE has made the measurement of strain and SR easier alongside its advantages in terms of angle interdependence by comparison with Doppler-based strain imaging. Although developed for the LV, STE has also been applied to the RV and even RA peak longitudinal strain. SR assessment is a factor independent from global cardiac function and motion and allows quantification of regional myocardial deformations in different RV segments (55-60). RV strain has been revealed to be reduced in patients with PAH, in patients after tetralogy of Fallot repair and systemic RV. However, strain values are influenced by loading situations. As has been proven in patients with PAH, RV longitudinal strain is correlated with systolic pulmonary artery pressure (61, 62). Furthermore, strain values are affected by RV size and also stroke volume. In addition, normal standard values for different ages, body sizes, and genders still have not been recognized and standardization between different software solutions is still being examined too. Accordingly, TDI and STE tools are not ready yet for daily and routine clinical practice (56-60). A global longitudinal RV free-wall 2D



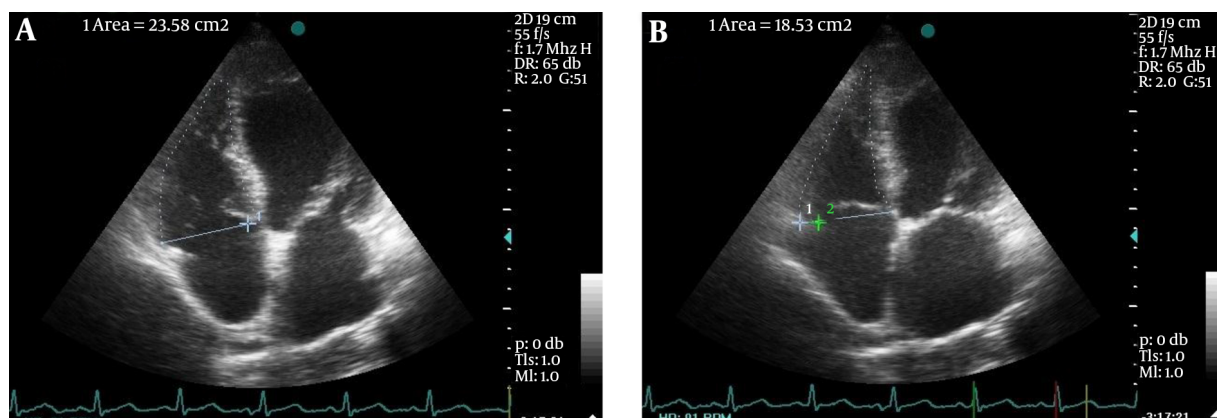


**Figure 2.** Showing Apical 4 Chamber RV Focused View in Diastole and Systole for Measurement of the RV FAC,  $RV\ FAC = (23.5 - 18.5) / 23.5 \times 100 = 21\%$

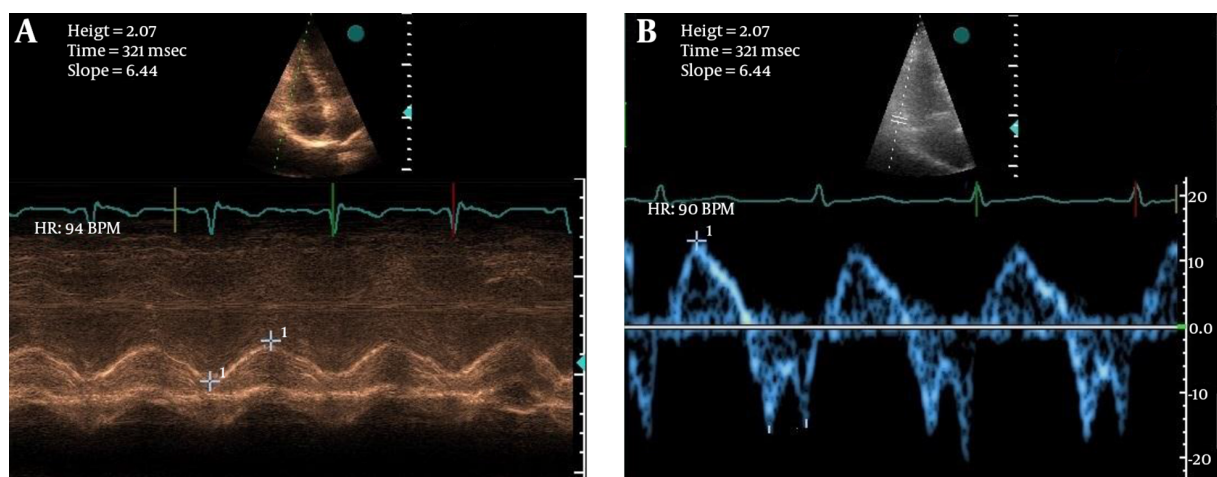


**Figure 3.** A, Tricuspid annular plane excursion (TAPSE) measured by M-mode from the end-diastole to the peak systole; B, Tricuspid annulus peak systolic velocity measured by the TDI (tissue Doppler imaging).

strain  $> -20\%$ , which means  $< 20\%$  in absolute value, has been suggested abnormal (40).

### 3.3.2. Right Ventricular Torsion

Ventricular torsion is its wringing motion around its longitudinal axis and not only does it contribute to both systolic and diastolic functions but also it defines stroke volume. Torsion by itself is the result of the contraction of the cardiac fibers arranged in a complex helical architecture with a prevalent oblique orientation and direction in the LV (right handed in the subendocardial and left handed in the subepicardial parts). Multiple studies using different modalities have examined the mechanics of LV torsion and its pattern in normal and pathologic situations (63-67). In contrast, RV fibers are chiefly oriented in longitudinal and circumferential directions, and there is a lack of infor-

mation on its torsional parameters. Pettersen et al. (68) used MRI tagging to assess RV apical and basal rotation in 14 healthy subjects as well as 14 patients with congenitally corrected transposition of the great arteries and revealed a counterclockwise rotation in RV apex and a clockwise rotation in RV base. Gustafsson et al. (69) studied RV apical rotation by STE in 14 healthy subjects and revealed a clockwise RV apical rotation but also reported a tightening belt motion for the RV with no effective rotation and torsion.

### 3.4. Evaluation of Right Ventricular Dyssynchrony

To study RV dyssynchrony, several groups are currently investigating specific electrocardiographic (QRS duration) and mechanical criteria of RV dyssynchrony. Echocardiographic indices of dyssynchrony are evaluated by measuring time delay in mechanical activity between the seg-

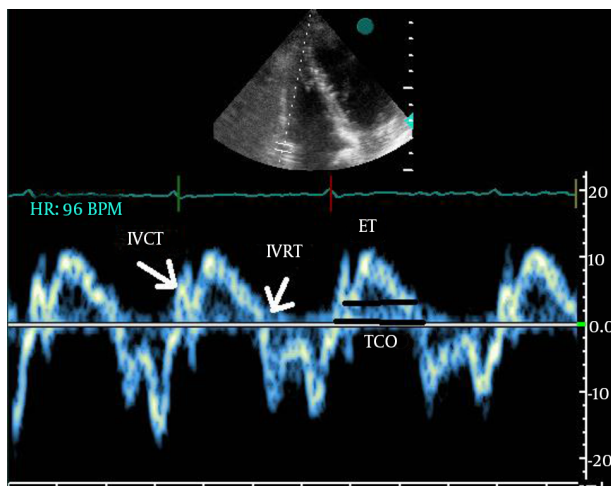


**Figure 4.** Calculation of RIMP (Right Ventricular Index of Myocardial Performance) by Pulse Tissue Doppler Imaging,  $RIMP = (TCO - ET) / ET$  or  $IVRT + IVCT/ET$

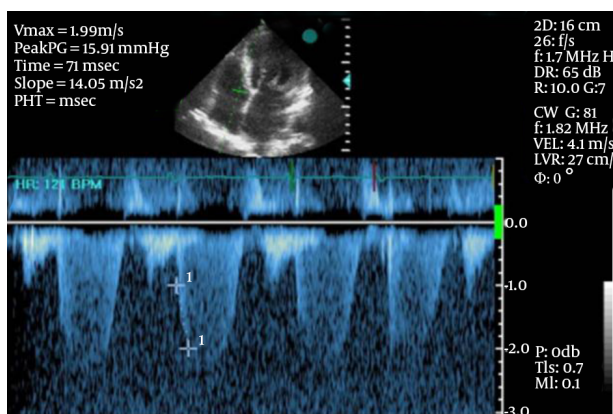


**Figure 5.** Showing dt 70 ms, or 0.07 Seconds Therefore RV dp/dt is About 12 mmHg/0.07 Seconds or 170 mmHg/s

ments. At this time, areas that can be assessed by tissue Doppler and STE are limited to the septum and RV free wall. Recently, 3D echocardiography and CMR have theoretically offered the advantage of assessing the 3D indices of dyssynchrony. Early after cardiac resynchronization therapy, RV mechanical delay can improve and a significant improvement is seen in patients with baseline RV mechanical dyssynchrony (70).

### 3.5. Three-Dimensional Echocardiography

Three-dimensional echocardiography allows accurate evaluation of the complex geometry and structure of RV chamber. It measures RV volumes and also EF globally without relying on geometric expectations. It thus

shows excellent relationships with CMR measurements in normal hearts and is able to discriminate pathology well (37, 71). New technological advances have made single heartbeat acquisitions possible. However, the main limitation of the new technique remains its dependence on a sufficient and satisfactory imaging window. Three-dimensional RVEF is particularly valuable in post cardiac surgery patients in whom TAPSE and  $S'$  are usually reduced (1).

RVEF measured by 3D echocardiography should be considered the method of quantifying RV systolic function in echo labs with the 3D platform. An RVEF < 45% usually indicates RV systolic dysfunction (40, 41).

### 3.6. Cardiovascular Magnetic Resonance

CMR is the second-line technique after echocardiography for a comprehensive RV study. CMR is presently considered the reference standard for functional RV assessment in that it allows for the visualization of the anatomy, quantification of the function, and also calculation of the flow (72). Anatomical evaluation is usually done with T1-weighted black-blood turbo spin-echo sequence or with the steady-state free precession (SSFP) sequence. Standard axial images permit segmental analysis of cardiac anatomy and visualization of the pulmonary veins, pulmonary arteries, aorta, and also all systemic veins. Detailed description of the intra- and extracardiac anatomy can be obtained by 3D rendering techniques, including contrast-enhanced magnetic resonance angiography and 3D SSFP. This is very important for a detailed description of a complex cardiac anatomy, especially in complex congenital heart disease and preoperative planning. CMR also provides an advanced imaging modality for an inclusive tissue characterization of RV myocardium. Technically, different T1- and T2-weighted sequences combined with late-enhancement imaging after gadolinium administration can be used for tissue characterization. Tissue characterization is employed for the study and differentiation of different cardiomyopathies affecting the RV such as arrhythmogenic RV cardiomyopathy, metabolic storage diseases, and cardiac tumors. Late enhancement imaging reveals intramyocardial fibrosis, inflammation, scars, and also fat accumulation. The prognostic significance of myocardial late-enhancement in various diseases needs further research. Regional RV function can be assessed qualitatively at rest and also during pharmacological stress on SSFP short-axis cine loops. Regional dysfunction can be evaluated quantitatively by using myocardial tagging or strain encoding CMR: Both techniques have been shown to be feasible in the RV and correlate well with advanced echocardiographic evaluation. However, their application in the RV is technically demanding owing to the thin wall

and extensive post-processing study, limiting their clinical routine application. Velocity-encoded phase-contrast imaging is another important CMR tool for RV evaluation. Phase-contrast imaging enables the quantification of RV stroke volume, pulmonary and tricuspid valve regurgitation, and intracardiac shunts (37, 71-75).

In congenital heart disease, the presence of myocardial scars in the RV is supposed to be a risk factor for a poor prognosis and adverse events during follow-up. RV volume and function assessment by CMR in patients with congenital heart disease has a major role in clinical decision-making specially in patients with severe pulmonary regurgitation after tetralogy of Fallot repair (76-80).

### 3.7. Multi-Detector Computed Tomography

Multi-detector computed tomography (MDCT) is not a technique normally used for RV study due to the important radiation exposure and the use of the iodinated contrast medium. MDCT is frequently performed when a concomitant or related thoracic or pulmonary disease, such as pulmonary embolism, is suspected. MDCT is a valued alternative to CMR in patients with pacemakers or CMR-incompatible prosthetic materials and also in patients suffering from claustrophobia. The use of MDCT for the RV has principally been validated for the detection of pulmonary embolism and for the workup of pulmonary hypertension (81, 82). Also, MDCT is increasingly used to detect coronary artery disease as its accuracy has been confirmed for the noninvasive visualization of all coronary arteries. Recently, the radiation dose has been significantly reduced, especially in comparison to diagnostic coronary angiography. Structural assessment of the RV by MDCT includes measurement of RV size and volumes, as well as RV free-wall thickness (RV hypertrophy). Based on the appropriate use criteria, CCT is appropriate for the evaluation of RV morphology and quantitative assessment of RV function. Septal bowing into the LV indicates RV volume (diastolic bowing to LV) or pressure overload (systolic bowing to LV).

### 3.8. Radionuclide Techniques

Historically, radionuclide techniques have been the first modalities used to study RV function. They have mostly been replaced by CMR, CCT, and echocardiography (35). Nevertheless, radionuclide techniques still play a role in the evaluation of RV myocardial ischemia, especially in patients in whom CMR is contraindicated. Among different modalities tested, gated blood-pool single-photon emission computed tomography (SPECT) is currently the suggested nuclear modality for quantifying RV function inasmuch as it overcomes the common limitations of

other nuclear techniques on the strength of its 3D nature. Gated SPECT is able to provide important RV volumetric and functional data. Also, radionuclide modalities are of additional special interest for assessing myocardial metabolism and perfusion. The usage of positron emission tomography or SPECT for RV study is generally limited by the low overall counts attributable to the RV compared with the LV, causing unreliable RV visualization. In the pathologic RV, hypertrophy leads to an increased RV mass and tracer uptake and results in better RV visualization. In PAH, changes in RV myocardial metabolism and perfusion are thought to be a precursor of the deterioration of systolic function, RV failure, and or clinical symptoms, and might be used for guiding management and decision making (83, 84).

### 3.9. Right-Heart Catheterization

The use of right-heart catheterization can create pressure-volume loops and confer a simultaneous study of the measurements of pressure and volume during each cardiac cycle. Varying pre- and afterload is used to define the end-diastolic and end-systolic pressure-volume relationships. The slope of the curve represents diastolic stiffness, which is the reciprocal of diastolic compliance. The latter, also referred to as end-systolic elastance, is a sensitive and virtually load- and heart-rate independent parameter of contractility. This technique, although deemed the gold standard method for assessing myocardial contractile status in animal experiments, is scarcely used in the clinic (1, 2, 9).

## 4. Conclusions

The RV is a complex structure that reveals important differences when compared to the LV. Morphologically, it cannot be described as a simple geometric form and functionally it is very sensitive to volume and pressure overload. Indeed, assessment of RV function, albeit difficult, has a major clinical importance in most cardiovascular diseases. So far, no single parameter has been proven to describe the functional status of the RV. Be that as it may, a combination of several parameters occasionally obtained through different imaging modalities and new techniques is needed to arrive at a clinically useful conclusion. Furthermore, RV dysfunction is an independent and important factor in the morbidity and mortality of cardiovascular disease.

## References

1. Haddad F, Hunt SA, Rosenthal DN, Murphy DJ. Right ventricular function in cardiovascular disease, part I anatomy, physiology, ag-



- ing, and functional assessment of the right ventricle. *Circulation*. 2008;**117**(11):1436-48.
2. Lee FA. Hemodynamics of the right ventricle in normal and disease states. *Cardiol Clin*. 1992;**10**(1):59-67. [PubMed: 1739960].
  3. Kukulski T, Hubbert L, Arnold M, Wranne B, Hatle L, Sutherland GR. Normal regional right ventricular function and its change with age: a Doppler myocardial imaging study. *J Am Soc Echocardiogr*. 2000;**13**(3):194-204. [PubMed: 10708468].
  4. Dias CA, Assad RS, Caneo LF, Abduch MC, Aiello VD, Dias AR, et al. Reversible pulmonary trunk banding. II. An experimental model for rapid pulmonary ventricular hypertrophy. *J Thorac Cardiovasc Surg*. 2002;**124**(5):999-1006. [PubMed: 12407385].
  5. Zaffran S, Kelly RG, Meilhac SM, Buckingham ME, Brown NA. Right ventricular myocardium derives from the anterior heart field. *Circ Res*. 2004;**95**(3):261-8. doi: 10.1161/01.RES.0000136815.73623.BE. [PubMed: 15217909].
  6. Dell'Italia LJ. The right ventricle: anatomy, physiology, and clinical importance. *Current Problems in Cardiology*. 1991;**16**(10):658-720. doi: 10.1016/0146-2806(91)90009-y.
  7. Jiang L. In: Right ventricle. Lippincott Williams Wilkins, editor. 38.; 1994.
  8. Goor DA, Lillehei CW. Congenital malformations of the heart: embryology, anatomy, and operative considerations. Grune & Stratton; 1975.
  9. Ho SY, Nihoyannopoulos P. Anatomy, echocardiography, and normal right ventricular dimensions. *Heart*. 2006;**92** Suppl 1:i2-13. doi: 10.1136/hrt.2005.077875. [PubMed: 16543598].
  10. McFadden DG, Barbosa AC, Richardson JA, Schneider MD, Srivastava D, Olson EN. The Hand 1 and Hand 2 transcription factors regulate expansion of the embryonic cardiac ventricles in a gene dosage-dependent manner. *Development*. 2005;**132**(1):189-201. doi: 10.1242/dev.01562. [PubMed: 15576406].
  11. Phan D, Rasmussen TL, Nakagawa O, McAnally J, Gottlieb PD, Tucker PW, et al. BOP, a regulator of right ventricular heart development, is a direct transcriptional target of MEF2C in the developing heart. *Development*. 2005;**132**(11):2669-78. doi: 10.1242/dev.01849. [PubMed: 15890826].
  12. Zeisberg EM, Ma Q, Juraszek AL, Moses K, Schwartz RJ, Izumo S, et al. Morphogenesis of the right ventricle requires myocardial expression of Gata4. *J Clin Invest*. 2005;**115**(6):1522-31. doi: 10.1172/JCI23769. [PubMed: 15902305].
  13. Molkenin JD, Kalvakolanu DV, Markham BE. Transcription factor GATA-4 regulates cardiac muscle-specific expression of the alpha-myosin heavy-chain gene. *Molecular and Cellular Biology*. 1994;**14**(7):4947-57. doi: 10.1128/mcb.14.7.4947.
  14. Small EM, Krieg PA. Transgenic analysis of the atrial natriuretic factor (ANF) promoter: Nkx2-5 and GATA-4 binding sites are required for atrial specific expression of ANF. *Developmental Biology*. 2003;**261**(1):116-31. doi: 10.1016/S0012-1606(03)00306-3.
  15. Lowes BD, Minobe W, Abraham WT, Rizeq MN, Bohlmeier TJ, Quaipe RA, et al. Changes in gene expression in the intact human heart. Downregulation of alpha-myosin heavy chain in hypertrophied, failing ventricular myocardium. *J Clin Invest*. 1997;**100**(9):2315-24. doi: 10.1172/JCI9770. [PubMed: 9410910].
  16. Sheehan F, Redington AN. The right ventricle: anatomy, physiology and clinical imaging. *Heart Vessels*. 2008;**94**:1510-5. doi: 10.1136/hrt.2007..
  17. Hayrapetyan H. Anatomical and physiological patterns of right ventricle. *J Cardiol Curr Res*. 2015;**2**(1).
  18. Santamore WP, Dell'Italia LJ. Ventricular interdependence: Significant left ventricular contributions to right ventricular systolic function. *Progress in Cardiovascular Diseases*. 1998;**40**(4):289-308. doi: 10.1016/S0033-0620(98)80049-2.
  19. Feneley MP, Gavaghan TP, Baron DW, Branson JA, Roy PR, Morgan JJ. Contribution of left ventricular contraction to the generation of right ventricular systolic pressure in the human heart. *Circulation*. 1985;**71**(3):473-80. [PubMed: 2578902].
  20. Chin KM, Kim NHS, Rubin LJ. The right ventricle in pulmonary hypertension. *Coronary Artery Disease*. 2005;**16**(1):13-8. doi: 10.1097/00019501-200502000-00003.
  21. Sandoval J, Bauerle O, Palomar A, Gomez A, Martinez-Guerra ML, Beltran M, et al. Survival in primary pulmonary hypertension. Validation of a prognostic equation. *Circulation*. 1994;**89**(4):1733-44. [PubMed: 8149539].
  22. McLaughlin VV, Sitbon O, Badesch DB, Barst RJ, Black C, Galie N, et al. Survival with first-line bosentan in patients with primary pulmonary hypertension. *Eur Respir J*. 2005;**25**(2):244-9. doi: 10.1183/09031936.05.00054804. [PubMed: 15684287].
  23. D'Alonzo GE, Barst RJ, Ayres SM, Bergofsky EH, Brundage BH, Detre KM, et al. Survival in patients with primary pulmonary hypertension. Results from a national prospective registry. *Ann Intern Med*. 1991;**115**(5):343-9. [PubMed: 1863023].
  24. Humbert M, Sitbon O, Yaici A, Montani D, O'Callaghan DS, Jais X, et al. Survival in incident and prevalent cohorts of patients with pulmonary arterial hypertension. *Eur Respir J*. 2010;**36**(3):549-55. doi: 10.1183/09031936.00057010. [PubMed: 20562126].
  25. Benza RL, Miller DP, Gomberg-Maitland M, Frantz RP, Foreman AJ, Coffey CS, et al. Predicting survival in pulmonary arterial hypertension: Insights from the registry to evaluate early and long-term pulmonary arterial hypertension disease management (reveal). *Circulation*. 2010;**122**(2):164-72. doi: 10.1161/CIRCULATIONAHA.109.898122. [PubMed: 20585012].
  26. Vonk Noordegraaf A, Galie N. The role of the right ventricle in pulmonary arterial hypertension. *Eur Respir Rev*. 2011;**20**(122):243-53. doi: 10.1183/09059180.00006511. [PubMed: 22130817].
  27. Hoeper MM, Barbera JA, Channick RN, Hassoun PM, Lang IM, Manes A, et al. Diagnosis, assessment, and treatment of non-pulmonary arterial hypertension pulmonary hypertension. *J Am Coll Cardiol*. 2009;**54**(1 Suppl):S85-96. doi: 10.1016/j.jacc.2009.04.008. [PubMed: 19555862].
  28. Lanzarini L, Fontana A, Campana C, Klersy C. Two simple echo-Doppler measurements can accurately identify pulmonary hypertension in the large majority of patients with chronic heart failure. *J Heart Lung Transplant*. 2005;**24**(6):745-54. doi: 10.1016/j.healun.2004.03.026. [PubMed: 15949736].
  29. Naeije R, Torbicki A. More on the noninvasive diagnosis of pulmonary hypertension: Doppler echocardiography revisited. *Eur Respir J*. 1995;**8**(9):1445-9. [PubMed: 8575567].
  30. Scapellato F, Temporelli PL, Eleuteri E, Corra U, Imparato A, Giannuzzi P. Accurate noninvasive estimation of pulmonary vascular resistance by Doppler echocardiography in patients with chronic heart failure. *J Am Coll Cardiol*. 2001;**37**(7):1813-9. doi: 10.1016/S0735-1097(01)01271-2.
  31. Konstantinides S, Geibel A, Olschewski M, Kasper W, Hruska N, Jackle S, et al. Importance of cardiac troponins I and T in risk stratification of patients with acute pulmonary embolism. *Circulation*. 2002;**106**(10):1263-8. [PubMed: 12208803].
  32. Torbicki A, Kurzyna M, Kuca P, Fijalkowska A, Sikora J, Florczyk M, et al. Detectable serum cardiac troponin T as a marker of poor prognosis among patients with chronic precapillary pulmonary hypertension. *Circulation*. 2003;**108**(7):844-8. doi: 10.1161/01.CIR.0000084544.54513.E2. [PubMed: 12900346].
  33. Kinch JW, Ryan TJ. Right ventricular infarction. *N Engl J Med*. 1994;**330**(17):1211-7. doi: 10.1056/NEJM199404283301707. [PubMed: 8139631].
  34. Haupt HM, Hutchins GM, Moore GW. Right ventricular infarction: role of the moderator band artery in determining infarct size. *Circulation*. 1983;**67**(6):1268-72. [PubMed: 6851021].
  35. Sugeng L, Mor-Avi V, Weinert L, Niel J, Ebner C, Steringer-Mascherbauer R, et al. Multimodality comparison of quantitative volumetric analysis of the right ventricle. *JACC Cardiovasc Imaging*. 2010;**3**(1):10-8. doi: 10.1016/j.jcmg.2009.09.017. [PubMed: 20129525].



36. Hammarstrom E, Wranne B, Pinto FJ, Puryear J, Popp RL. Tricuspid Annular Motion. *J Am Soc Echocardiogr*. 1991;4(2):131-9. doi: [10.1016/s0894-7317\(14\)80524-5](https://doi.org/10.1016/s0894-7317(14)80524-5).
37. Leibundgut G, Rohner A, Grize L, Bernheim A, Kessel-Schaefer A, Bremerich J, et al. Dynamic assessment of right ventricular volumes and function by real-time three-dimensional echocardiography: a comparison study with magnetic resonance imaging in 100 adult patients. *J Am Soc Echocardiogr*. 2010;23(2):116-26. doi: [10.1016/j.echo.2009.11.016](https://doi.org/10.1016/j.echo.2009.11.016). [PubMed: 20152692].
38. Sadeghpour A, Shahrahi M, Bakhshandeh H, Naderi N. Normal Echocardiographic Values of 368 Iranian Healthy Subjects. *Arch Cardiovasc Imag*. 2013;1(2):72-9. doi: [10.5812/acvi.15662](https://doi.org/10.5812/acvi.15662).
39. Shojaeifard M, Esmailzadeh M, Maleki M, Bakhshandeh H, Parvaresh F, Naderi N. Normal reference values of tissue Doppler imaging parameters for right ventricular function in young adults: a population based study. *Res Cardiovasc Med*. 2013;2(4):160-6. doi: [10.5812/cardiovascmed.9843](https://doi.org/10.5812/cardiovascmed.9843). [PubMed: 25478514].
40. Lang RM, Badano LP, Mor-Avi V, Afilalo J, Armstrong A, Ernande L, et al. Recommendations for cardiac chamber quantification by echocardiography in adults: an update from the American Society of Echocardiography and the European Association of Cardiovascular Imaging. *J Am Soc Echocardiogr*. 2015;28(1):1-39 e14. doi: [10.1016/j.echo.2014.10.003](https://doi.org/10.1016/j.echo.2014.10.003). [PubMed: 25559473].
41. Rudski LG, Lai WW, Afilalo J, Hua L, Handschumacher MD, Chandrasekaran K, et al. Guidelines for the echocardiographic assessment of the right heart in adults: A report from the american society of echocardiography endorsed by the european association of echocardiography, a registered branch of the european society of cardiology, and the canadian society of echocardiography. 23. ; 2010.
42. Tei C, Dujardin KS, Hodge DO, Bailey KR, McGoon MD, Tajik AJ, et al. Doppler echocardiographic index for assessment of global right ventricular function. *J Am Soc Echocardiogr*. 1996;9(6):838-47. doi: [10.1016/s0894-7317\(96\)90476-9](https://doi.org/10.1016/s0894-7317(96)90476-9).
43. Ueti OM, Camargo EE, Ueti Ade A, de Lima-Filho EC, Nogueira EA. Assessment of right ventricular function with Doppler echocardiographic indices derived from tricuspid annular motion: comparison with radionuclide angiography. *Heart*. 2002;88(3):244-8. [PubMed: 12181215].
44. Eidem BW, Tei C, O'Leary PW, Cetta F, Seward JB. Nongeometric quantitative assessment of right and left ventricular function: Myocardial performance index in normal children and patients with Ebstein anomaly. *J Am Soc Echocardiogr*. 1998;11(9):849-56. doi: [10.1016/s0894-7317\(98\)70004-5](https://doi.org/10.1016/s0894-7317(98)70004-5).
45. Yeo T, Dujardin KS, Tei C, Mahoney DW, McGoon MD, Seward JB. Value of a Doppler-Derived Index Combining Systolic and Diastolic Time Intervals in Predicting Outcome in Primary Pulmonary Hypertension. *Am J Cardiol*. 1998;81(9):1157-61. doi: [10.1016/s0002-9149\(98\)00140-4](https://doi.org/10.1016/s0002-9149(98)00140-4).
46. Vogel M, Schmidt MR, Kristiansen SB, Cheung M, White PA, Sorensen K, et al. Validation of myocardial acceleration during isovolumic contraction as a novel noninvasive index of right ventricular contractility: comparison with ventricular pressure-volume relations in an animal model. *Circulation*. 2002;105(14):1693-9. [PubMed: 11940549].
47. Stein PD, Sabbah HN, Anbe DT, Marzilli M. Performance of the failing and nonfailing right ventricle of patients with pulmonary hypertension. *Am J Cardiol*. 1979;44(6):1050-5. doi: [10.1016/0002-9149\(79\)90168-1](https://doi.org/10.1016/0002-9149(79)90168-1).
48. Brimioules S, Wauthy P, Ewalenko P, Rondelet B, Vermeulen F, Kerbaul F, et al. Single-beat estimation of right ventricular end-systolic pressure-volume relationship. *Am J Physiol Heart Circ Physiol*. 2003;284(5):H1625-30. doi: [10.1152/ajpheart.01023.2002](https://doi.org/10.1152/ajpheart.01023.2002). [PubMed: 12531727].
49. Kanzaki H, Nakatani S, Kawada T, Yamagishi M, Sunagawa K, Miyatake K. Right ventricular dp/dt/P(max), not dp/dt(max), noninvasively derived from tricuspid regurgitation velocity is a useful index of right ventricular contractility. *J Am Soc Echocardiogr*. 2002;15(2):136-42. [PubMed: 11836488].
50. Singbal Y, Vollbon W, Huynh LT, Wang WY, Ng AC, Wahi S. Exploring Noninvasive Tricuspid dp/dt as a Marker of Right Ventricular Function. *Echocardiography*. 2015;32(9):1347-51. doi: [10.1111/echo.12877](https://doi.org/10.1111/echo.12877). [PubMed: 25556710].
51. Sadeghpour A, Harati H, Kiavar M, Esmaeizadeh M, Maleki M, et al. Correlation of right ventricular dp/dt with functional capacity and RV function in patients with mitral stenosis. *icrj*. 2008;1(4):208-219.
52. Fujii J, Yazaki Y, Sawada H, Aizawa T, Watanabe H, Kato K. Noninvasive assessment of left and right ventricular filling in myocardial infarction with a two-dimensional Doppler echocardiography method. *J Am Coll Cardiol*. 1985;5(5):1155-60. doi: [10.1016/s0735-1097\(85\)80018-8](https://doi.org/10.1016/s0735-1097(85)80018-8).
53. Yanase O, Motomiya T, Tejima T, Nomura S. Doppler echocardiographic assessment of right ventricular filling characteristics in hemodynamically significant right ventricular infarction. *Am J Noninvasiv Cardiol*. 1992;6(4):230-6.
54. Yilmaz M, Erol MK, Acikel M, Sevimli S, Alp N. Pulsed Doppler tissue imaging can help to identify patients with right ventricular infarction. *Heart Vessels*. 2003;18(3):112-6. doi: [10.1007/s00380-003-0703-2](https://doi.org/10.1007/s00380-003-0703-2). [PubMed: 12955425].
55. Maffessanti F, Gripari P, Tamborini G, Muratori M, Fusini L, Alamanni F, et al. Evaluation of right ventricular systolic function after mitral valve repair: a two-dimensional Doppler, speckle-tracking, and three-dimensional echocardiographic study. *J Am Soc Echocardiogr*. 2012;25(7):701-8. doi: [10.1016/j.echo.2012.03.017](https://doi.org/10.1016/j.echo.2012.03.017). [PubMed: 22542273].
56. Unsworth B, Casula RP, Kyriacou AA, Yadav H, Chukwuemeka A, Cherian A, et al. The right ventricular annular velocity reduction caused by coronary artery bypass graft surgery occurs at the moment of pericardial incision. *Am Heart J*. 2010;159(2):314-22. doi: [10.1016/j.ahj.2009.11.013](https://doi.org/10.1016/j.ahj.2009.11.013). [PubMed: 20152232].
57. Kowalski M, Kukulski T, Jamal F, D'hooge J, Weidemann F, Rademakers F, et al. Can natural strain and strain rate quantify regional myocardial deformation? A study in healthy subjects. *Ultrasound Med Biol*. 2001;27(8):1087-97. doi: [10.1016/s0301-5629\(01\)00388-x](https://doi.org/10.1016/s0301-5629(01)00388-x).
58. Haghighi ZO, Alizadehasl A, Maleki M, Naderi N, Esmaeilzadeh M, Noohi F, et al. Echocardiographic Assessment of Right Atrium Deformation Indices in Healthy Young Subjects. *Am Heart J*. 2013;1(1):2-7.
59. Jamal F, Bergerot C, Argaud L, Loufouat J, Ovide M. Longitudinal strain quantitates regional right ventricular contractile function. *Am J Physiol Heart Circ Physiol*. 2003;285(6):H2842-7. doi: [10.1152/ajp-heart.00218.2003](https://doi.org/10.1152/ajp-heart.00218.2003). [PubMed: 12893635].
60. Weidemann F, Jamal F, Sutherland GR, Claus P, Kowalski M, Hatle L, et al. Myocardial function defined by strain rate and strain during alterations in inotropic states and heart rate. *Am J Physiol Heart Circ Physiol*. 2002;283(2):H792-9. doi: [10.1152/ajpheart.00025.2002](https://doi.org/10.1152/ajpheart.00025.2002). [PubMed: 12124229].
61. Sadeghpour A, Kyavar M, Madadi S, Ebrahimi L, Khajali Z, Alizadeh Sani Z. Doppler-derived strain and strain rate imaging assessment of right ventricular systolic function in adults late after tetralogy of Fallot repair: an observational study. *Anatolian J Cardiol*. 2013 doi: [10.5152/akd.2013.174](https://doi.org/10.5152/akd.2013.174).
62. Scherptong RW, Mollema SA, Blom NA, Kroft LJ, de Roos A, Vliegen HW, et al. Right ventricular peak systolic longitudinal strain is a sensitive marker for right ventricular deterioration in adult patients with tetralogy of Fallot. *Int J Cardiovasc Imaging*. 2009;25(7):669-76. doi: [10.1007/s10554-009-9477-7](https://doi.org/10.1007/s10554-009-9477-7). [PubMed: 19642012].
63. van der Hulst AE, Delgado V, Holman ER, Kroft LJ, de Roos A, Hazekamp MG, et al. Relation of left ventricular twist and global strain with right ventricular dysfunction in patients after operative "correction" of tetralogy of fallot. *Am J Cardiol*. 2010;106(5):723-9. doi: [10.1016/j.amjcard.2010.04.032](https://doi.org/10.1016/j.amjcard.2010.04.032). [PubMed: 20723653].
64. Nagel E, Stuber M, Burkhard B, Fischer SE, Scheidegger MB, Boesiger P, et al. Cardiac rotation and relaxation in patients with aortic valve stenosis. *Eur Heart J*. 2000;21(7):582-9. [PubMed: 10775013].
65. Sandstede JJ, Johnson T, Harre K, Beer M, Hofmann S, Pabst T,

- et al. Cardiac systolic rotation and contraction before and after valve replacement for aortic stenosis: a myocardial tagging study using MR imaging. *AJR Am J Roentgenol.* 2002;**178**(4):953-8. doi: [10.2214/ajr.178.4.1780953](https://doi.org/10.2214/ajr.178.4.1780953). [PubMed: [11906882](https://pubmed.ncbi.nlm.nih.gov/11906882/)].
66. Ojaghi-Haghighi Z, Alizadehasl A, Hashemi A. Reverse Left Ventricular Apical Rotation in Dilated Cardiomyopathy. *Arch Cardiovasc Imag.* 2015;**3**(2) doi: [10.5812/acvi.28112](https://doi.org/10.5812/acvi.28112).
  67. Russel IK, Götte MJW, Bronzwaer JG, Knaapen P, Paulus WJ, van Rossum AC. Left ventricular torsion: an expanding role in the analysis of myocardial dysfunction. *JACC.* 2009;**2**(5):648-55.
  68. Pettersen E, Helle-Valle T, Edvardsen T, Lindberg H, Smith HJ, Smevik B, et al. Contraction pattern of the systemic right ventricle shift from longitudinal to circumferential shortening and absent global ventricular torsion. *J Am Coll Cardiol.* 2007;**49**(25):2450-6. doi: [10.1016/j.jacc.2007.02.062](https://doi.org/10.1016/j.jacc.2007.02.062). [PubMed: [17599609](https://pubmed.ncbi.nlm.nih.gov/17599609/)].
  69. Gustafsson U, Lindqvist P, Waldenström A. Apical circumferential motion of the right and the left ventricles in healthy subjects described with speckle tracking. *J Am Soc Echocardiogr.* 2008;**21**(12):1326-30. doi: [10.1016/j.echo.2008.09.014](https://doi.org/10.1016/j.echo.2008.09.014). [PubMed: [19041576](https://pubmed.ncbi.nlm.nih.gov/19041576/)].
  70. Esmaeilzadeh M, Poorzand H, Maleki M, Sadeghpour A, Parsaee M. Evaluation of Longitudinal Right Ventricular Mechanical Dyssynchrony before and Early after Cardiac Resynchronization Therapy: A Strain Imaging Study. *J Tehran Heart Cent.* 2011;**6**(1):24-30. [PubMed: [23074601](https://pubmed.ncbi.nlm.nih.gov/23074601/)].
  71. Shimada YJ, Shiota M, Siegel RJ, Shiota T. Accuracy of right ventricular volumes and function determined by three-dimensional echocardiography in comparison with magnetic resonance imaging: a meta-analysis study. *J Am Soc Echocardiogr.* 2010;**23**(9):943-53. doi: [10.1016/j.echo.2010.06.029](https://doi.org/10.1016/j.echo.2010.06.029). [PubMed: [20797527](https://pubmed.ncbi.nlm.nih.gov/20797527/)].
  72. Geva T. Is MRI the preferred method for evaluating right ventricular size and function in patients with congenital heart disease?: MRI is the preferred method for evaluating right ventricular size and function in patients with congenital heart disease. *Circ Cardiovasc Imaging.* 2014;**7**(1):190-7. doi: [10.1161/CIRCIMAGING.113.000553](https://doi.org/10.1161/CIRCIMAGING.113.000553). [PubMed: [24449548](https://pubmed.ncbi.nlm.nih.gov/24449548/)].
  73. Balluz R, Liu L, Zhou X, Ge S. Real Time Three-Dimensional Echocardiography for Quantification of Ventricular Volumes, Mass, and Function in Children with Congenital and Acquired Heart Diseases. *Echocardiography.* 2013;**30**(4):472-82. doi: [10.1111/echo.12132](https://doi.org/10.1111/echo.12132).
  74. Oosterhof T, Tulevski I, Vliegen HW, Spijkerboer AM, Mulder BJ. Effects of volume and/or pressure overload secondary to congenital heart disease (tetralogy of fallot or pulmonary stenosis) on right ventricular function using cardiovascular magnetic resonance and B-type natriuretic peptide levels. *Am J Cardiol.* 2006;**97**(7):1051-5. doi: [10.1016/j.amjcard.2005.10.047](https://doi.org/10.1016/j.amjcard.2005.10.047). [PubMed: [16563914](https://pubmed.ncbi.nlm.nih.gov/16563914/)].
  75. Tandri H, Macedo R, Calkins H, Marcus F, Cannon D, Scheinman M, et al. Role of magnetic resonance imaging in arrhythmogenic right ventricular dysplasia: insights from the North American arrhythmogenic right ventricular dysplasia (ARVD/C) study. *Am Heart J.* 2008;**155**(1):147-53. doi: [10.1016/j.ahj.2007.08.011](https://doi.org/10.1016/j.ahj.2007.08.011). [PubMed: [18082506](https://pubmed.ncbi.nlm.nih.gov/18082506/)].
  76. Greutmann M, Tobler D, Biaggi P, Mah ML, Crean A, Oechslin EN, et al. Echocardiography for assessment of right ventricular volumes revisited: a cardiac magnetic resonance comparison study in adults with repaired tetralogy of Fallot. *J Am Soc Echocardiogr.* 2010;**23**(9):905-11. doi: [10.1016/j.echo.2010.06.013](https://doi.org/10.1016/j.echo.2010.06.013). [PubMed: [20667695](https://pubmed.ncbi.nlm.nih.gov/20667695/)].
  77. Sadeghpour A, Kyavar M, Alizadehasl A. Springer: Verlag London; 2014. Comprehensive Approach to Adult Congenital Heart Disease.
  78. Perloff JK, Child JS, Aboulhosn J. Congenital heart disease in adults. Elsevier Health Sciences; 2009.
  79. Allen HD, Driscoll DJ, Shaddy RE, Feltes TF. Moss and Adams heart disease in infants, children, and adolescents: Including the fetus and young adult. Lippincott Williams & Wilkins; 2013.
  80. Oechslin EN, Harrison DA, Harris L, Downar E, Webb GD, Siu SS, et al. Reoperation in adults with repair of tetralogy of fallot: Indications and outcomes. *J Thorac Cardiovasc Surg.* 1999;**118**(2):245-51. doi: [10.1016/S0022-5223\(99\)70214-X](https://doi.org/10.1016/S0022-5223(99)70214-X).
  81. Taylor AJ, Cerqueira M, Hodgson JM, Mark D, Min J, O'Gara P, et al. Appropriate use criteria for cardiac computed tomography. *J Am Coll Cardiol.* 2010;**56**(22):1864-94. doi: [10.1016/j.jacc.2010.07.005](https://doi.org/10.1016/j.jacc.2010.07.005). [PubMed: [21087721](https://pubmed.ncbi.nlm.nih.gov/21087721/)].
  82. Hakim H, Samadikhah J, Alizadehasl A, Azarfarin R. Chronobiological rhythms in onset of massive pulmonary embolism in Iranian population. *Middle East J Anesthesiol.* 2009;**20**:369-75.
  83. Pfisterer ME, Battler A, Zaret BL. Range of normal values for left and right ventricular ejection fraction at rest and during exercise assessed by radionuclide angiography. *Eur Heart J.* 1985;**6**(8):647-55. [PubMed: [4054134](https://pubmed.ncbi.nlm.nih.gov/4054134/)].
  84. Greil GF, Beerbaum P, Razavi R, Miller O. Imaging the right ventricle: non-invasive imaging. *Heart.* 2008;**94**(6):803-8. doi: [10.1136/hrt.2005.079111](https://doi.org/10.1136/hrt.2005.079111). [PubMed: [18480359](https://pubmed.ncbi.nlm.nih.gov/18480359/)].